

# Synthesis of mono substituted asymmetrical (*E*)-1-(1-(pyridin-2-yl)ethylidene)thiocarbonohydrazide: Structural characterization and antioxidant activity study

Cheikh Ndoye<sup>a</sup>, Aissatou Alioune Gaye<sup>a</sup>, Alioune Fall<sup>a</sup>, Ousmane Diouf<sup>a</sup>,  
Mohamed Gaye<sup>a,\*</sup>

<sup>a</sup>Department of Chemistry; University Cheikh Anta DIOP de Dakar, Senegal

\*Corresponding author at: Mohamed Gaye

---

**Abstract:** A new dissymmetrical ligand (*E*)-1-(1-(pyridin-2-yl)ethylidene)thiocarbonohydrazide (**1**) by a monocondensation reaction of thiocarbonohydrazone with 2-acetylpyridine. The compound was characterized by physico-chemical analyses, elemental analyses, FTIR, <sup>1</sup>H and <sup>13</sup>C NMR spectroscopy techniques. The structure of the (**1**) was determined by single-crystal X-ray diffraction study. The compound (C<sub>8</sub>H<sub>11</sub>N<sub>5</sub>S) crystallizes in the monoclinic space group *Pbca* with the following unit cell parameters: *a* = 10.8365 (2) Å, *b* = 7.7659 (2) Å, *c* = 24.8771 (5) Å, *V* = 2093.54 (8) Å<sup>3</sup>, *Z* = 8, *R*<sub>1</sub> = 0.028, *wR*<sub>2</sub> = 0.116. The crystal packing of compound (**1**) is stabilized by intermolecular hydrogen bonds which form layers parallel to *ac* plane. The thiocarbonohydrazide moiety C=N-N-C(S)-N-NH<sub>2</sub> is almost planar. The dihedral angle between the mean planes of the pyridine ring and the thiocarbonohydrazide moiety is 6.69°. The antioxidant activities of the two compounds were investigated.

**Keywords:** Thiocarbonohydrazone, 2-acetylpyridine, X-ray.

---

Date of Submission: 13-02-2022

Date of Acceptance: 28-02-2022

---

## I. Introduction

Thiocarbonohydrazide (H<sub>2</sub>NNHC(S)NHNH<sub>2</sub>) is a compound with two identical arms that are very reactive towards carbonyl compounds. It is possible to make only one of the arms react or both by scrupulously controlling the reaction conditions. Parameters that need to be controlled are the thiocarbonohydrazide/carbonyl ratio, the dilution, and the method of addition of the reagents [1–5]. This control gives access by monocondensation to monosubstituted compounds, or to symmetrical or unsymmetrical compounds by di-condensation. Both thiocarbonohydrazide and its homologous carbonohydrazide have been widely studied in this last decades [6–12]. Their derivatives are used as precursors in heterocycle chemistry [13–15]. The compounds resulting from these precursors are studied for their biological properties and for the development of drugs [16–19]. They are known to possess a wide spectrum of biological activities such as antioxidant [20], analgesic [21], antiplatelet [22], antimicrobial [23], anticonvulsant [24], antifungal [25], antidepressant [26], anti-tuberculosis [27], anti-diabetics [28,29] and anti-cancer [30,31]. The molecules formed from carbonohydrazide or thiocarbonohydrazide form a class of multitopic ligands which are used in the preparation of coordination compounds with atypical structures, possessing original properties [11,32–34]. As part of our search for a suitable ligand for the construction of metal complex gates, we prepared (*E*)-1-(1-(pyridin-2-yl)ethylidene)thiocarbonohydrazide (**1**), a structural analogue of a series of carbonohydrazide derivatives which proved to be good ligands for developing original organometallic structures [11,12,35,36]. Herein, we report the synthesis and crystal structure of a monocondensed thiocarbonohydrazide derivative (**1**) whose antioxidant activity has been investigated.

## II. Experimental

### 2.1. Starting materials and Instrumentations

2-acetylpyridine, 2-hydroxy-3-methoxybenzaldehyde, as well as thiocarbonohydrazide were commercial products (from Aldrich) and were used without further purification. Solvents were of reagent grade and were purified by the usual methods. Elemental analyses of C, H and N were recorded on a VxRio EL Instrument. Infrared spectra were obtained on an FTIR Spectrum Two of Perkin Elmer spectrometer in the

---

\*Corresponding author: mohamedl.gaye@ucad.edu.sn

4000-400 cm<sup>-1</sup> region. The <sup>1</sup>H NMR spectra were recorded at 300 MHz and <sup>13</sup>C{<sup>1</sup>H} NMR spectra at 75 MHz on a Bruker AC-300 instrument.

### 2.2. Synthesis of (E)-1-(1-(pyridin-2-yl)ethylidene)thiocarbonohydrazide (1)

The procedure is inspired by the method reported by Novaket *et al* [37], with some modification. Herein, 2-acetylpyridine was used instead of salicylaldehyde. To a mixture of 20 mL of methanol and 10 mL of distilled water was added thiocarbonohydrazide (2 g, 0.0188 mol) at room temperature. A solution of 2-acetylpyridine (2.114 mL, 0.0188 mmol) dissolved in 20 mL of methanol was slowly added dropwise over a period of one hour. The resulting mixture was heated under reflux for 3 h. The suspension was filtered, and the white precipitate obtained was washed with 2 × 10 mL of hot methanol and dried under vacuum over P<sub>2</sub>O<sub>5</sub>. M.p.: 197°C. Yield: 75.6 % Analytical for (1) C<sub>8</sub>H<sub>11</sub>N<sub>5</sub>S: Calc (found) % C = 45.81 (45.91); H = 5.25 (5.30); N = 33.42 (33.47); S = 15.29 (15.32). IR (ν, cm<sup>-1</sup>): 3263, 3165, 1577, 1531, 1498, 1459, 1431, 1218. <sup>1</sup>H NMR (500 MHz, dms<sub>o</sub>-d<sub>6</sub>, δ, ppm): 2.37 (s, 3H, -CH<sub>3</sub>), 4.99 (s, 2H, -NH<sub>2</sub>), 7.38-8.51 (m, 4H, H<sub>Py</sub>), 9.92 (s, 1H, -NH), 10.30 (s, 1H, -NH). <sup>13</sup>C NMR (125 MHz, dms<sub>o</sub>-d<sub>6</sub>, δ, ppm): 176.53 (C=S), 155.29 (C<sub>ipso</sub>), 148.72 (CH<sub>3</sub>-C=N), 148.44 (C<sub>Py</sub>), 136.77 (C<sub>Py</sub>), 124.20 (C<sub>Py</sub>), 121.46 (C<sub>Py</sub>), 12.43 (CH<sub>3</sub>-C=N-). UV-Vis (DMF, λ<sub>max</sub> (nm)): 314 nm.

### 2.3. Free radical scavenging antioxidant assay

Antioxidant capacities of compound (1) is measured according to Akhtar *et al.* [38] method with some modifications. 3.8 mL of the methanol solution of DPPH• (40 mg/L) was added to test compound (200 μL) at different concentrations. The mixture was shaken vigorously and incubated in dark for 30 min at room temperature. After the incubation time, the absorbance of the solution was measured at 517 nm by using Lamda 365 UV-vis spectrophotometer Perkin Elmer. The DPPH• radical scavenger effect was calculated using the following equation:

$$\text{Scavenging activity (\% control)} = \frac{A_{\text{control}} - A_{\text{sample}}}{A_{\text{control}}} \times 100$$

where  $A_{\text{control}}$  is the absorbance of the control reaction and  $A_{\text{sample}}$  is the absorbance of the test compound. The tests were carried out in triplicate. TROLOX was used as positive control.

### 2.4. X-ray data collection, structure determination, and refinement

The details of the X-ray crystal structure solution and refinement are given in Table 1. Measurements were made on a SuperNova Rigaku Oxford Diffraction diffractometer. Data collection reduction and multiscan ABSPACK correction were performed with CrysAlisPro (Rigaku Oxford Diffraction). Using Olex2 [39] the structures were solved by intrinsic phasing methods with SHELXT [40] and SHELXL [41] was used for full matrix least squares refinement. All H-atoms were found experimentally and their coordinates and  $U_{\text{iso}}$  parameters were constraint to 1.5  $U_{\text{eq}}$  for the methyl group and to 1.2  $U_{\text{eq}}$  for the other atoms.

**Table 1.** Crystal data and structure refinement for (1).

Chemical formula	C <sub>8</sub> H <sub>11</sub> N <sub>5</sub> S
$M_r$	209.28
Crystal shape/color	Prism/colorless
Crystal system, Space group	Orthorhombic, <i>Pbca</i>
Crystal size (mm)	0.2 × 0.06 × 0.02
$a$ (Å)	10.8365 (2),
$b$ (Å)	7.7659 (2)
$c$ (Å)	24.8771 (5)
$V$ (Å <sup>3</sup> )	2093.54 (8)
$Z$	8
$D_{\text{calc}}$ (g.cm <sup>-3</sup> )	1.328
Cu $K\alpha$ (Å)	1.54184
$T$ (K)	295
$\mu$ (mm <sup>-1</sup> )	2.51
Index ranges	-8 ≤ $h$ ≤ 13, -9 ≤ $k$ ≤ 9, -30 ≤ $l$ ≤ 27
$F(000)$	880
$\theta$ range (°)	3.553-72.914
No. of measured reflections	7548
Independent reflections	2045
Observed [ $I > 2\sigma(I)$ ] reflections	1798

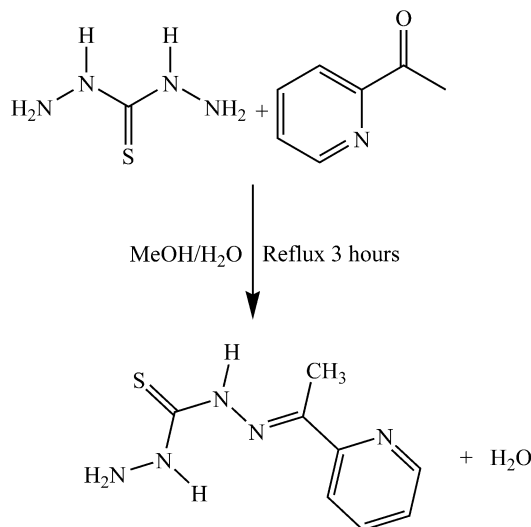
$R_{int}$	0.028
$R[F^2 > 2\sigma(F^2)]$	0.040
$wR(F^2)$	0.116
Goodness-of-fit (GOF) on $F^2$	1.05
No. of parameters	140
No. of restraints	0
$\Delta\rho_{max}, \Delta\rho_{min}$ (e $\text{\AA}^{-3}$ )	0.27, -0.19

### III. Results And Discussion

#### 3.1. General study

The elemental analyses results are in accordance with the chemical formulae expected from the reaction scheme 1. The infrared spectrum of compound exhibits broad band pointed at  $3263\text{ cm}^{-1}$  which are attributed to  $\text{NH}_2$  stretching [42]. The vibration of the imine functions appears at  $1577\text{ cm}^{-1}$  while the band due to C=S group is pointed out at  $1218\text{ cm}^{-1}$  as reported for similar Schiff base [43,44]. Bands due to the aromatic ring are pointed in the region  $1531\text{-}1431\text{ cm}^{-1}$ .

The  $^1\text{H}$  and  $^{13}\text{C}$  NMR spectra of the compound were recorded in  $\text{dms}\text{-d}_6$ . The  $^1\text{H}$  NMR spectrum (Figure 1) of the compound **1** reveals a signal at 2.37 ppm attributed to the proton of the  $-\text{CH}_3$  group and a signal at 4.99 ppm assigned to the protons of the  $-\text{NH}_2$  moiety [10,45]. The multiplet appearing in the range 7.38-8.51 ppm is representative of the aromatic protons. The signals at 9.92 and 10.30 ppm are attributed to the two different  $-\text{NH}$  of the dissymmetry compound [46]. These observations are in accordance with the  $^{13}\text{C}$  spectrum of compound (Figure 2). The signal at 148.72 ppm attributed to the C=N is indicative of the successful of the condensation reaction. The signals of the methyl carbon atom and the thiocarbonyl carbon atom appear respectively at 12.43 ppm and  $\delta$  176.53 ppm. Additional signals are pointed for the aromatic carbon atoms in the range 148.44-121.46 ppm. The attribution of these signals is confirmed by the NMR sequence 135 DEPT which allows to discriminate the carbons according to the number of protons present on the carbon atom. Indeed, the signals representing the quaternary carbon atoms do not appear in the 135 DEPT spectrum. The  $-\text{CH}$  and  $\text{CH}_3$  signals appear in opposite directions (Figure 3). In the electronic spectrum of the ligand the strong band which appears at 314 nm is due to the intraligand  $n\rightarrow\pi^*$  transitions of the C=N chromophore (Figure 4).



Scheme 1. Synthesis procedure of (1).

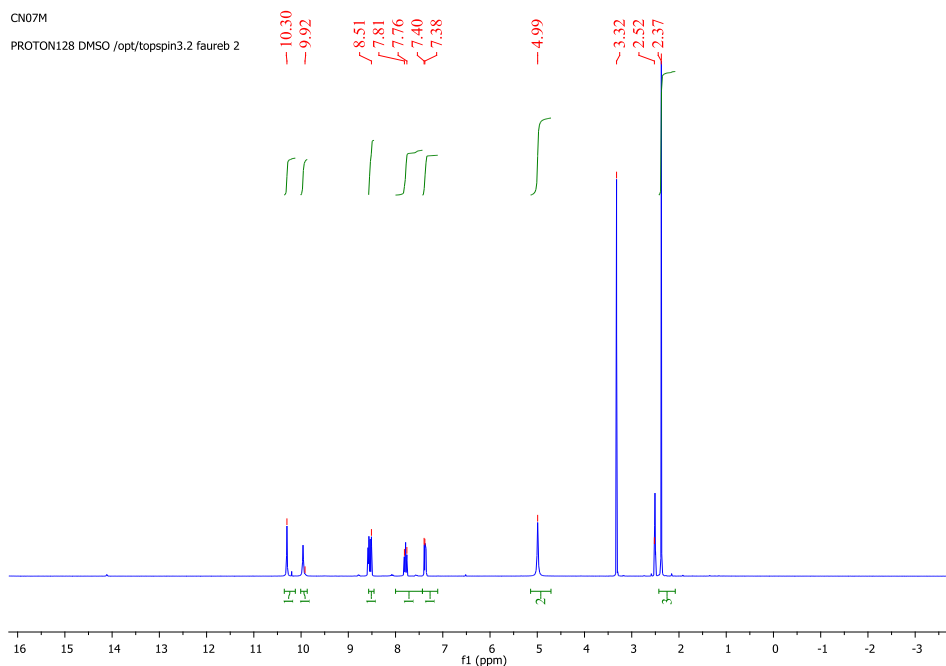


Figure 1 :  $^1\text{H}$  NMR of compound (1).

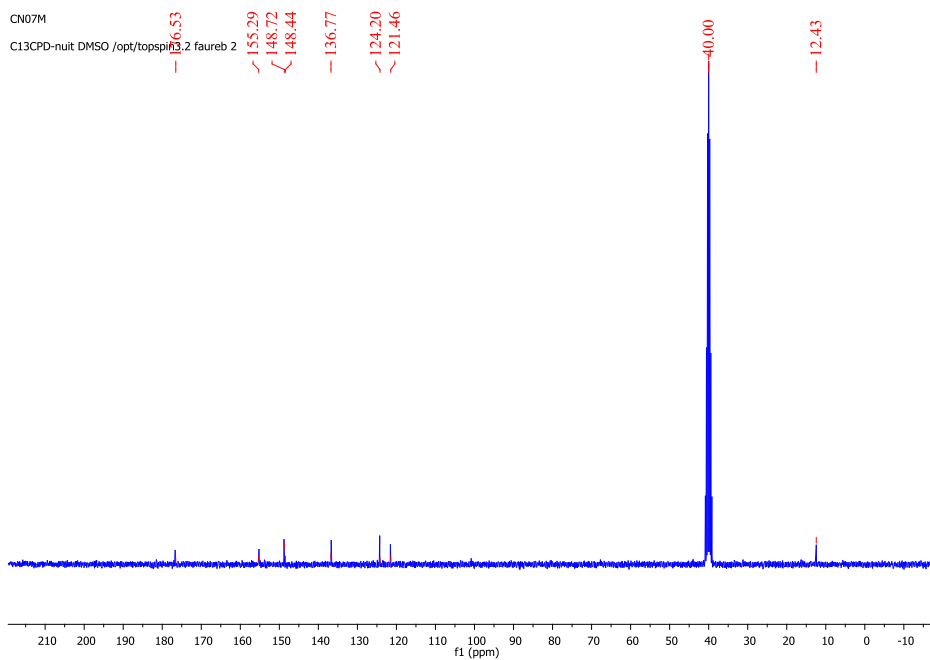


Figure 2 :  $^{13}\text{C}$  NMR of (1).

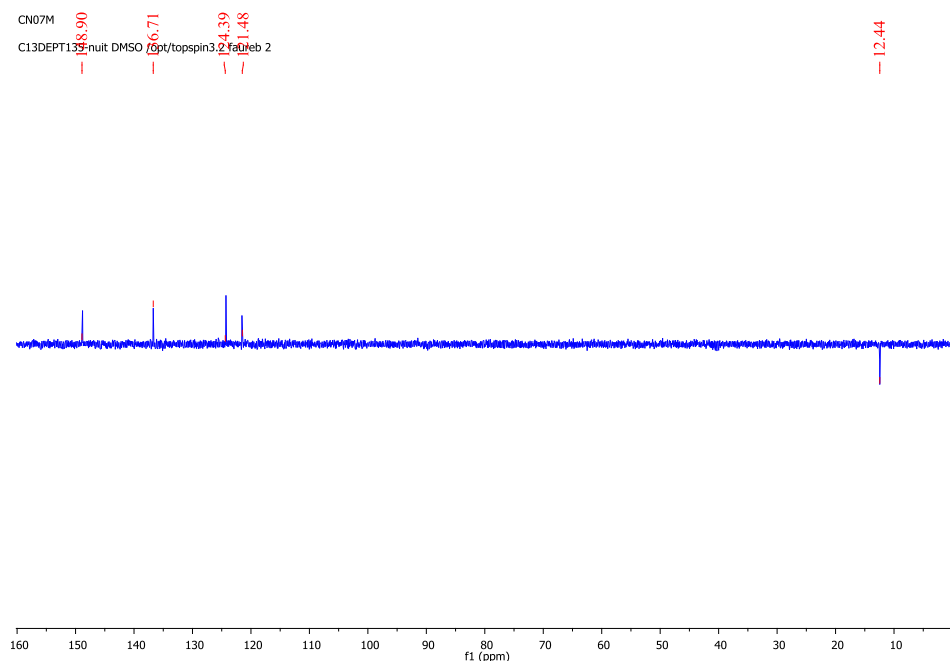


Figure 3 :  $^{13}\text{C}$  DEPT 135 of (1).

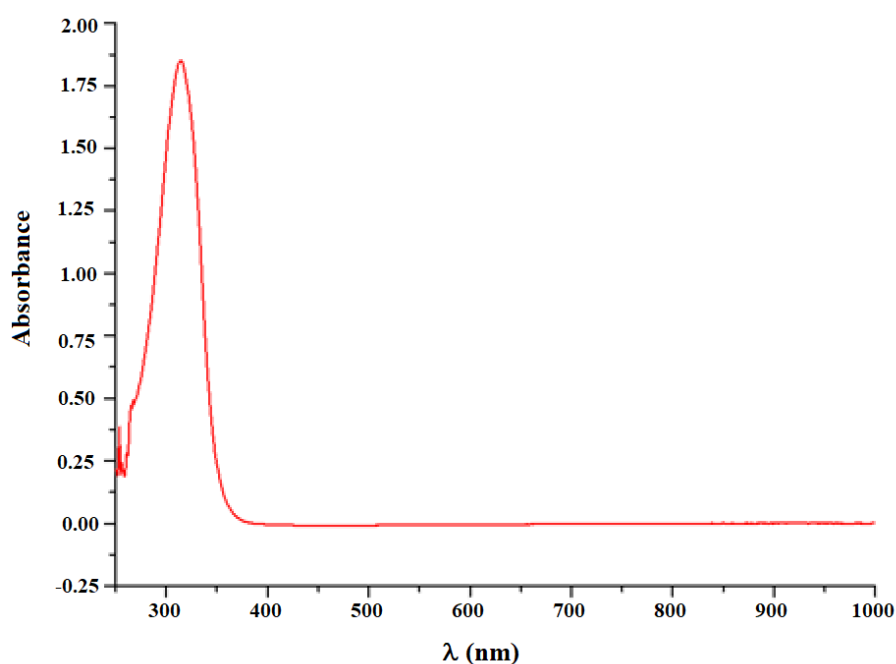


Figure 4 : Electronic spectrum of (1).

### 3.2. Description of crystal structure of ligand

Suitable X-ray diffraction crystal of (1) were obtained by slow evaporation of corresponding methanol solution. The compound (1) crystallizes in the orthorhombic system with a *Pbca* space group. The asymmetric unit contains one dissymmetrical organic molecule of **1**. The molecular structure with the atomic-labelling is shown in Figure 5. The selected bond lengths and bond angles are listed in Table 2. The crystal structure reveals that the Schiff base adopts the thioketo form, as showed by the bond length of 1.6878(16) Å for C1—S1 which is compatible with a double bond character [43,47]. The C2—N4 have double bond character with the distance value of 1.286 (2) Å. The values of 1.329 (2) Å and 1.347 (2) Å are indicative of single bond character for C1—N2 and C1—N3 respectively [48,49]. The bond lengths of 1.404 (2) Å and 1.3749 (18) Å for N1—N2 and N3—N4 respectively are indicative of single bond character. These values are comparable to those reported for the compound 2-[(*E*)-2-{2-[(*E*)-2-Hydroxybenzylidene]hydrazinocarbonyl}hydrazinylidene)methyl]phenol

[50]. The molecule adopts an *E* configuration with respect to C2=N4 bond. The S1 atom of the thiocarbonyl moiety and the -NH<sub>2</sub> are in *syn* conformation with respect to the C1—N2 bond while the S1 and the N4 atom are in *trans* with respect to the C1—N3. In fact, the torsion angle values of -1.1(2)° [S1—C1—N2—N1] and 176.4(1)° [S1—C1—N3—N4] are compatible with these observations. The thiocarbonohydrazide moiety C=N-N-C(S)-N-NH<sub>2</sub> is almost planar (rms 0.0211 Å) with a maximum deviation from least-squares plane of 0.0304(1) Å for the N3 atom. The torsion angles values of -1.1(2)° [N1—N2—C1—S1], 176.4(1)° [S1—C1—N3—N4], -179.3(1)° [C2—N4—N3—C1], 178.5(1)° [N1—N2—C1—N3] and -3.3(2)° [N4—N3—C1—N2] are in accordance with the above observation. The pyridine ring N1/C3-C7 and the thiocarbonohydrazide moiety N1—N2—C1(S)—N3—N4—C2 are almost coplanar with dihedral angle between their mean planes of 6.692(1)°.

In the crystal of (1), two types of intermolecular hydrogen-bonding are observed (Table 4). The first type is constituted by the N3—H3···N1 hydrogen bond between the hydrazinyl moiety of the condensed arm of the thiocarbonohydrazide and the amino group of the uncondensed hydrazide moiety, the N2—H2···S1 hydrogen bond between the hydrazinyl moiety of the uncondensed hydrazide moiety and the sulfur atom of the thiocarbonohydrazide and the hydrogen bond N1—H1A···S1 the amino group of the uncondensed hydrazide moiety and the sulfur atom. The secondary hydrogen-bonding type is formed by C4—H4···S1. The intermolecular hydrogen bonds, N3—H3···N1<sup>i</sup> (*i*:  $x-1/2, -y+3/2, -z+1$ ), N2—H2···S1<sup>ii</sup> (*ii*:  $x+1/2, -y+3/2, -z+1$ ), and N1—H1A···S1<sup>iii</sup> (*iii*:  $-x+1/2, y+1/2, z$ ) lead to the formation of layers parallel to *ac* plan (Fig. 6, Table 4). The layers are linked by the C4—H4···S1<sup>ii</sup> (*ii*:  $x+1/2, -y+3/2, -z+1$ ).

**Table 2.** Selected bond lengths (Å) and angles (°) for the (1).

S1—C1	1.6878 (16)	N5—C7	1.340 (3)
N3—N4	1.3749 (18)	C3—C2	1.489 (2)
N3—C1	1.347 (2)	C3—C4	1.385 (3)
N4—C2	1.286 (2)	C2—C8	1.491 (2)
N2—N1	1.404 (2)	C4—C5	1.383 (3)
N2—C1	1.329 (2)	C5—C6	1.370 (4)
N5—C3	1.335 (2)	C6—C7	1.365 (4)
C1—N3—N4	118.67 (12)	C4—C3—C2	121.45 (16)
C2—N4—N3	118.32 (13)	N4—C2—C3	115.17 (15)
C1—N2—N1	123.24 (14)	N4—C2—C8	125.60 (14)
C3—N5—C7	117.15 (18)	N2—C1—S1	122.17 (12)
N3—C1—S1	120.69 (11)	N2—C1—N3	117.14 (14)

**Table 4.** Hydrogen-bond geometry (Å, °)

<i>D</i> —H··· <i>A</i>	<i>D</i> —H	H··· <i>A</i>	<i>D</i> ··· <i>A</i>	<i>D</i> —H··· <i>A</i>
N3—H3···N1 <sup>i</sup>	0.86	2.21	3.049(2)	166.5
N2—H2···S1 <sup>ii</sup>	0.86	2.66	3.3780(14)	142.2
C4—H4···S1 <sup>ii</sup>	0.96(3)	2.67 (3)	3.561(2)	155(2)
N1—H1A···S1 <sup>iii</sup>	0.90(3)	2.74 (3)	3.634(2)	172(3)

Symmetry codes: (i)  $x-1/2, -y+3/2, -z+1$ ; (ii)  $x+1/2, -y+3/2, -z+1$ ; (iii)  $-x+1/2, y+1/2, z$ .

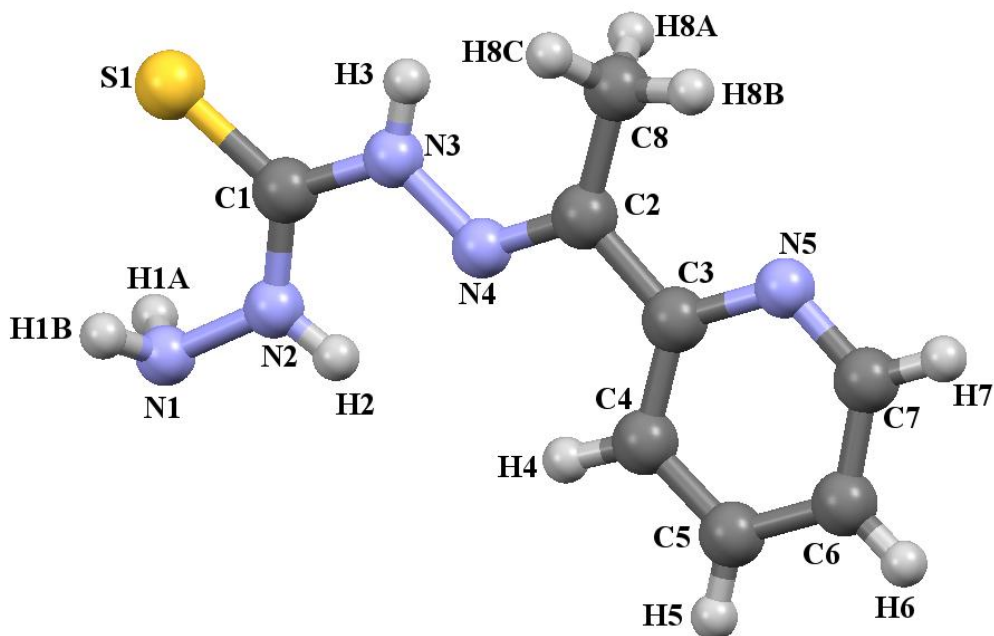


Figure 5 : The crystal structure of the compound.

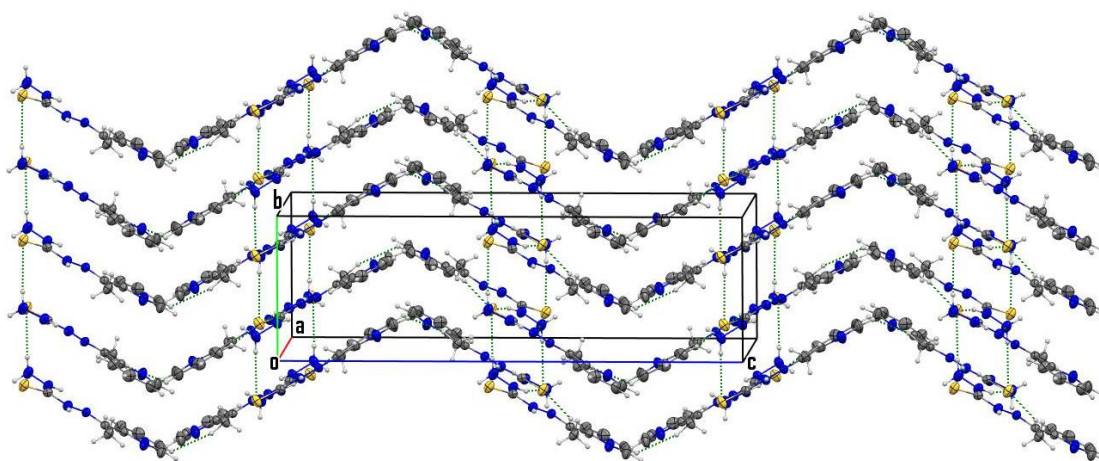


Figure 6 : Layers of compound viewed along the *ac* plan

### 3.3. Antioxidant activity

The DPPH<sup>•</sup> radical scavenging method is widely used to assess the antioxidant activity of various compounds. In fact, DPPH<sup>•</sup> is a stable free radical which becomes a stable molecule when it accepts an electron or a hydrogen radical. The scavenging effects of the compound 1 and of the control (TROLOX) were evaluated (Table 5, Figure 7) by varying the concentration of DPPH<sup>•</sup> (0.1014 and 0.0507 mM), and the concentration of TROLOX and that of compound (1) (100–500 μM). Figure 7 shows plots of DPPH<sup>•</sup> free radical scavenging activity (%) for TROLOX and compound (1). It appears that the scavenging activity of compound (1) increases significantly with increasing concentration in the range tested (100–500 μM) for the two initial concentrations of DPPH<sup>•</sup>. The scavenging activity of (1) varies, for the highest concentration of DPPH<sup>•</sup> (0.1014 mM), between 9.02±0.09 % and 47.26±0.24 % and between 19.60±0.29 % and 57.02± 0.67 % for the lowest concentration of DPPH<sup>•</sup> (0.0507 mM). This activity is due to the NH hydrazinyl groups which can react with the DPPH<sup>•</sup> radical by the typical H abstraction reaction to form a stable radical. For the highest concentration of DPPH<sup>•</sup>, the measurements show that the activity of TROLOX is comparable to that of compound (1) in the concentration range examined with inhibition percentages between 12.25±0.09 % and 51.38±0.09 % for TROLOX and 9.02±0.09 % and 47.26±0.24 % for (1). For the lowest concentration of DPPH<sup>•</sup>, a strong increase in the scavenging activity of compound (1) is observed, which exhibits an IC<sub>50</sub> at the concentration of 438.65 μM. At

the concentration of 100  $\mu\text{M}$  the compound is more active than TROLOX with respective inhibition percentages of  $19.60 \pm 0.29$  and  $12.01 \pm 0.73\%$ . Between 100 and 500  $\mu\text{M}$ , TROLOX becomes more active than compound (1) with inhibition percentages which vary respectively between  $36.62 \pm 0.24 - 94.57 \pm 0.62\%$  and  $25.86 \pm 0.19 - 57.02 \pm 0.67\%$ .

**Table 4.** Antioxidant activity of (1) at different concentration of DPPH<sup>•</sup>.

Concentration ( $\mu\text{M}$ )	[DPPH <sup>•</sup> ] = 0.1014 mM		[DPPH <sup>•</sup> ] = 0.0507 mM	
	Trolox	(1)	Trolox	(1)
100	$12.25 \pm 0.09$	$9.02 \pm 0.09$	$12.01 \pm 0.73$	$19.60 \pm 0.29$
200	$18.33 \pm 0.09$	$21.05 \pm 0.38$	$36.62 \pm 0.24$	$25.86 \pm 0.19$
300	$32.54 \pm 0.11$	$27.89 \pm 0.31$	$56.80 \pm 0.10$	$39.08 \pm 0.19$
400	$43.08 \pm 0.15$	$37.51 \pm 0.09$	$82.23 \pm 0.43$	$45.40 \pm 0.19$
500	$51.38 \pm 0.09$	$47.26 \pm 0.24$	$94.57 \pm 0.62$	$57.02 \pm 0.67$

We studied the effect of the initial concentration of DPPH<sup>•</sup> on the % of DPPH<sup>•</sup> remaining over time. Figure 8 shows the variation of the % of DPPH<sup>•</sup> consumed during the reaction between DPPH<sup>•</sup> and compound (1). The decrease in absorbance was followed for 240 min. After this time, the highest concentration of remaining DPPH<sup>•</sup> was observed for the highest initial DPPH<sup>•</sup> concentration, whereas a decrease in the initial concentration of DPPH<sup>•</sup> shows a lowering of remaining DPPH<sup>•</sup>. These results, clearly demonstrate that a decrease in the concentration of DPPH<sup>•</sup> accelerates its consumption by compound (1). As shown in Figure 8 after 45 min, 80% of the lowest concentration of DPPH<sup>•</sup> were consumed, while less of 60% remains for the highest initial concentration of DPPH<sup>•</sup>. It appears clearly in Figure 8 that the maximum consumption of DPPH<sup>•</sup> is reached after 45 min for the lowest concentration, whereas for the highest DPPH<sup>•</sup> concentration the consumption continues for up to 240 min. It should be noted that the consumption of DPPH<sup>•</sup> in the reaction with compound (1) is very fast at the start of the reaction, in both cases.

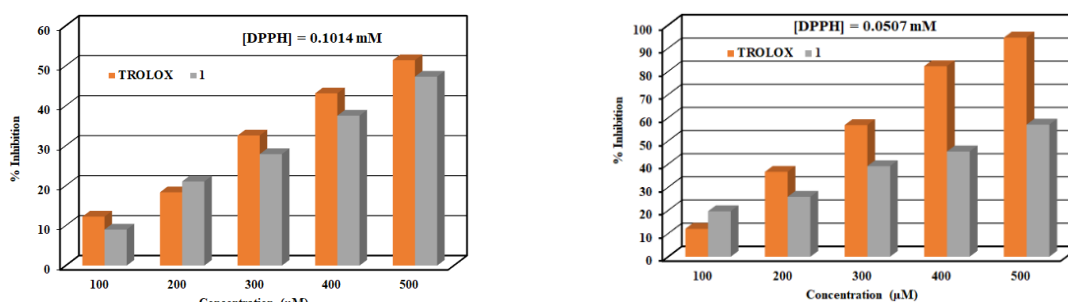


**Figure 7.** Antioxidant activity of (1) : [DPPH<sup>•</sup>] = 0.1014 mM and [DPPH<sup>•</sup>] = 0.0507 mM.

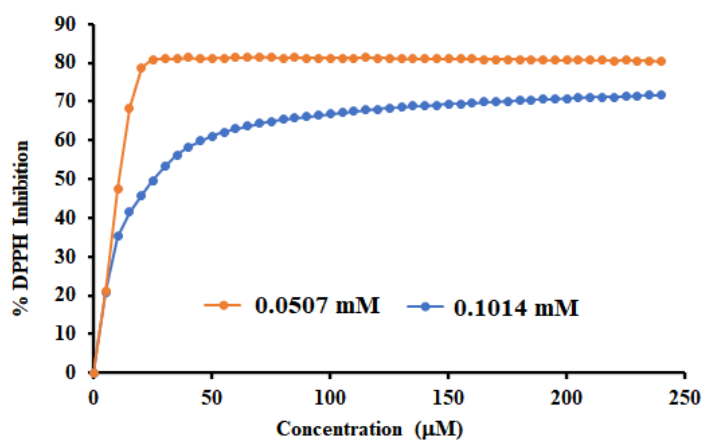


**Figure 8.** Percentage of remaining DPPH<sup>•</sup> during the reaction of DPPH<sup>•</sup> with compound (1). Analyses were performed with two DPPH<sup>•</sup> concentrations 0.0507 mM and 0.1014 mM.



#### IV. Conclusion

The monosubstituted thiocarbonohydrazide derivative (E)-1-(1-(pyridin-2-yl)ethylidene)thiocarbonohydrazide (**1**) was successfully synthesized and its structure was confirmed by elemental analysis and spectroscopic techniques (FT-IR, <sup>1</sup>H and <sup>13</sup>C NMR). The molecular structure of (**1**) is determined by X-ray diffraction technique. The monosubstituted derivative shows good antioxidant activity comparatively to the antioxidant activity of TROLOX. Compound (**1**) at 500 μM, showed moderate antioxidant activity of about 47.26-57.02 % for the different DPPH\* concentrations used in this study. The kinetic study shows that the maximum consumption of DPPH\* is reached after 45 min for the 0.0507 mM concentration, whereas for the 0.1014 the consumption continues for up to 240 min.

#### Supplementary Materials:

CCDC-2152489 contains the supplementary crystallographic data for this paper. These data can be obtained free of charge via <https://www.ccdc.cam.ac.uk/structures/>, or by e-mailing [data\\_request@ccdc.cam.ac.uk](mailto:data_request@ccdc.cam.ac.uk), or by contacting The Cambridge Crystallographic Data Centre, 12 Union Road, Cambridge CB2 1EZ, UK; fax: +44(0)1223-336033.

#### References

- [1]. M.U. Kumar, A.P. Jeyakumari, M. Suresh, S. Chandran, G. Vinitha, Synthesis, spectroscopic and DFT studies of Schiff based (E)-N'-(Benzo[d][1,3]Dioxol-5-ylmethylene)nicotinohydrazide monohydrate single crystal: a promising organic nonlinear optical material, *Mater. Res. Express*, 2019, 6, 075102.
- [2]. S. Sivaraman, A. Agilandewari, C. Balakrishnan, R.M. Sockalingam, S.P. Meenakshisundaram, R. Markkandan, Supramolecular architecture and computational studies of nicotinohydrazide and furan-2-carbohydrazide crystals, *J. Mol. Struct.*, 2018, 1173, 385–397.
- [3]. Z.T. Omar Al-Ahdal, S. Jadhav, M. Rai, Potentiometric and Thermodynamic Studies of (N-[-(4-Chlorophenyl)Methylene]Nicotinohydrazide) and Its Transition Metal Complexes, *Integ. Ferroelectr.*, 2020, 205, 88–94.
- [4]. A. Bacchi, M. Carcelli, G. Pelizzi, C. Solinas, L. Sorace, Trinuclear copper(II) complexes of bis(acylhydrazone) ligands. Structural analysis and magnetic properties of a sulfato-bridged hexanuclear dimer, *Inorg. Chim. Acta*, 2006, 359, 2275–2280.
- [5]. S. Liu, L. Gelmini, S.J. Rettig, R.C. Thompson, C. Orvig, Synthesis and characterization of lanthanide [Ln(L)]<sub>2</sub> complexes of N<sub>4</sub>O<sub>3</sub> amine phenol ligands with phenolate oxygen bridges: evidence for very weak magnetic exchange between lanthanide ions, *J. Am. Chem. Soc.*, 1992, 114, 6081–6087.
- [6]. B. Čobeljić, I. Turel, A. Pevec, Z. Jagličić, D. Radanović, K. Anđelković, M.R. Milenković, Synthesis, structures and magnetic properties of octahedral Co(III) complexes of heteroaromatic hydrazones with tetrakisothiocyanato Co(II) anions, *Polyhedron*, 2018, 155, 425–432.
- [7]. Z. Moussa, M. Al-Mamary, S. Al-Juhani, S.A. Ahmed, Preparation and biological assessment of some aromatic hydrazones derived from hydrazides of phenolic acids and aromatic aldehydes, *Heliyon*, 2020, 6, e05019.
- [8]. B.S.K. Aktar, Y. Sıcak, T.T. Tok, E.E. Oruç-Emre, A.Ş. Yağlıoğlu, A.K. İyidoğan, M. Öztürk, I. Demirtaş, Designing heterocyclic chalcones, benzoyl/sulfonyl hydrazones: An insight into their biological activities and molecular docking study, *J. Mol. Struct.*, 2020, 1211, 128059.
- [9]. I.A. Khodja, H. Boulebd, C. Bensouici, A. Belfaitah, Design, synthesis, biological evaluation, molecular docking, DFT calculations and in silico ADME analysis of benzimidazole-hydrazone derivatives as promising antioxidant, antifungal, and anti-acetylcholinesterase agents, *J. Mol. Struct.*, 2020, 1218, 128527.
- [10]. T.M. Seck, F.D. Faye, A.A. Gaye, I.E. Thiam, O. Diouf, M. Gaye, P. Retailleau, Synthesis of mono and bis-substituted asymmetrical compounds, (1-(pyridin-2-yl)ethylidene)carbonohydrazide and 1-(2'-hydroxybenzylidene)-5-(1'-pyridylethylidene)carbonohydrazone: Structural characterization and antioxidant activity study, *Eur. J. Chem.*, 2020, 11, 285–290.
- [11]. T.M. Seck, M. Diop, D. Diouf, O. Diouf, A.H. Barry, M. Gaye, Synthesis, spectroscopic studies and crystal structure determination of a tetranuclear Zn(II) [2x2] square grid structure of 1,5-bis(1-(pyridin-2-yl)ethylidene)carbonohydrazide, *J. Appl. Chem.*, 2018, 11, 06–14.
- [12]. T.M. Seck, P.A. Gaye, C. Ndoye, I.E. Thiam, O. Diouf, P. Retailleau, M. Gaye, Diaquabis{μ-1,5-bis[(pyridin-2-yl)methylidene]carbonohydrazide(1-)}di-μ-chlorido-tetra-chloridotetrazinc(II), *Acta Crystallogr., Sect. E: Struct. Chem.*, 2020, 76, 1349–1352.
- [13]. Y.-Y. Wu, W.-B. Shao, J.-J. Zhu, Z.-Q. Long, L.-W. Liu, P.-Y. Wang, Z. Li, S. Yang, Novel 1,3,4-Oxadiazole-2-carbohydrazides as Prospective Agricultural Antifungal Agents Potentially Targeting Succinate Dehydrogenase, *J. Agric. Food Chem.*, 2019, 67, 13892–13903.
- [14]. Y. Liu, H. Song, Y. Huang, J. Li, S. Zhao, Y. Song, P. Yang, Z. Xiao, Y. Liu, Y. Li, H. Shang, Q. Wang, Design, Synthesis, and Antiviral, Fungicidal, and Insecticidal Activities of Tetrahydro-β-carboline-3-carbohydrazide Derivatives, *J. Agric. Food Chem.*, 2014, 62, 9987–9999.
- [15]. Z. Huang, Y. Liu, Y. Li, L. Xiong, Z. Cui, H. Song, H. Liu, Q. Zhao, Q. Wang, Synthesis, Crystal Structures, Insecticidal Activities, and Structure–Activity Relationships of Novel N'-tert-Butyl-N'-substituted-benzoyl-N-[di(octa)hydro]benzofuran{(2,3-dihydro)benzo[1,3]([1,4])dioxine)carbohydrazide Derivatives, *J. Agric. Food Chem.*, 2011, 59, 635–644.
- [16]. M. Zia-ur-Rehman, J.A. Choudary, M.R.J. Elsegood, H.L. Siddiqui, K.M. Khan, A facile synthesis of novel biologically active 4-hydroxy-N'-(benzylidene)-2H-benzo[e][1,2]thiazine-3-carbohydrazide 1,1-dioxides, *Eur. J. Med. Chem.*, 2009, 44, 1311–1316.
- [17]. J. Camacho, A. Barazarte, N. Gamboa, J. Rodrigues, R. Rojas, A. Vaisberg, R. Gilman, J. Charris, Synthesis and biological evaluation of benzimidazole-5-carbohydrazide derivatives as antimalarial, cytotoxic and antitubercular agents, *Bioorg. Med. Chem.*, 2011, 19, 2023–2029.
- [18]. B. Parrino, S. Ullo, A. Attanzio, S. Cascioferro, V. Spanò, A. Carbone, A. Montalbano, P. Barraja, G. Cirrincione, L. Tesoriere, P. Diana, Synthesis of 5H-pyrido[3,2-b]pyrrolizin-5-one tripeptone analogs with antitumor activity, *Eur. J. Med. Chem.*, 2018, 158, 236–246.
- [19]. C.R.D. Silva, J. Wang, M.D. Carducci, S.A. Rajapakshe, Z. Zheng, Synthesis, structural characterization and luminescence studies of a novel europium(III) complex [Eu(DBM)<sub>3</sub>(TPTZ)] (DBM: dibenzoylmethanate; TPTZ: 2,4,6-tri(2-pyridyl)-1,3,5-triazine), *Inorg. Chim. Acta*, 2004, 357, 630–634.

- [20]. M. Demurtas, A. Baldisserotto, I. Lampronti, D. Moi, G. Balboni, S. Pacifico, S. Vertuani, S. Manfredini, V. Onnis, Indole derivatives as multifunctional drugs: Synthesis and evaluation of antioxidant, photoprotective and antiproliferative activity of indole hydrazones, *Bioorg. Chem.* 2019, 85, 568–576.
- [21]. L. Zhang, L. Shi, S.M. Soars, J. Kamps, H. Yin, Discovery of Novel Small-Molecule Inhibitors of NF- $\kappa$ B Signaling with Antiinflammatory and Anticancer Properties, *J. Med. Chem.*, 2018, 61, 5881–5899.
- [22]. S.S. Bharadwaj, B. Poojary, S.K.M. Nandish, J. Kengaiyah, M.P. Kirana, M.K. Shankar, A.J. Das, A. Kulal, D. Sannaningaiah, Efficient Synthesis and in Silico Studies of the Benzimidazole Hybrid Scaffold with the Quinolinoyloxadiazole Skeleton with Potential  $\alpha$ -Glucosidase Inhibitory, Anticoagulant, and Antiplatelet Activities for Type-II Diabetes Mellitus Management and Treating Thrombotic Disorders, *ACS Omega*, 2018, 3, 12562–12574.
- [23]. K.D. Kataraya, S.R. Shah, D. Reddy, Anticancer, antimicrobial activities of quinoline based hydrazone analogues: Synthesis, characterization and molecular docking, *Bioorg. Chem.*, 2020, 94, 103406.
- [24]. L. Dehestani, N. Ahangar, S.M. Hashemi, H. Irannejad, P.H. Masihi, A. Shakiba, S. Emami, Design, synthesis, in vivo and in silico evaluation of phenacyl triazole hydrazones as new anticonvulsant agents, *Bioorg. Chem.*, 2018, 78, 119–129.
- [25]. A.-E. Dascalu, A. Ghinet, E. Lipka, C. Furman, B. Rigo, A. Fayeulle, M. Billamboz, Design, synthesis and evaluation of hydrazine and acyl hydrazone derivatives of 5-pyrrolidin-2-one as antifungal agents, *Bioorg. Med. Chem. Lett.*, 2020, 30, 127220.
- [26]. A.B. Thomas, R.K. Nanda, L.P. Kothapalli, S.C. Hamane, Synthesis and biological evaluation of Schiff's bases and 2-azetidiones of isonocotiny hydrazone as potential antidepressant and nootropic agents, *Arab. J. Chem.*, 2016, 9, S79–S90.
- [27]. P. Rawat, R.N. Singh, P. Niranjana, A. Ranjan, N.R.F. Holguín, Evaluation of antituberculosis activity and DFT study on dipyrromethane-derived hydrazone derivatives, *J. Mol. Struct.*, 2017, 1149, 539–548.
- [28]. K. Karrouchi, S. Fattach, M.M. Jotani, A. Sagaama, S. Radi, H.A. Ghabbour, Y.N. Mabkhot, B. Himmi, M.E.A. Faouzi, N. Issaoui, Synthesis, crystal structure, hirshfeld surface analysis, DFT calculations, anti-diabetic activity and molecular docking studies of (E)-N<sup>2</sup>-(5-bromo-2-hydroxybenzylidene) isonicotinohydrazide, *J. Mol. Struct.*, 2020, 1221, 128800.
- [29]. J.B. Wright, W.E. Dulin, J.H. Markillie, The Antidiabetic Activity of 3,5-Dimethylpyrazoles, *J. Med. Chem.*, 1964, 7, 102–105.
- [30]. D. Das Mukherjee, N.M. Kumar, M.P. Tantak, A. Das, A. Ganguli, S. Datta, D. Kumar, G. Chakrabarti, Development of Novel Bis(indolyl)-hydrazide-Hydrazone Derivatives as Potent Microtubule-Targeting Cytotoxic Agents against A549 Lung Cancer Cells, *Biochemistry*, 2016, 55, 3020–3035.
- [31]. S. Narayanan, P. Gupta, U. Nazim, M. Ali, N. Karadkhelkar, M. Ahmad, Z.-S. Chen, Anti-cancer effect of Indanone-based thiazolyl hydrazone derivative on colon cancer cell lines, *The Int. J. Biochem. Cell Biol.*, 2019, 110, 21–28.
- [32]. M.U. Anwar, K.V. Shuvaev, L.N. Dawe, L.K. Thompson, Polynuclear Fen Complexes (n = 1, 2, 4, 5) of Polytopic Hydrazone Ligands with Fe(II), Fe(III) and Mixed Oxidation State Combinations, *Inorg. Chem.*, 2011, 50, 12141–12154.
- [33]. L.N. Dawe, K.V. Shuvaev, L.K. Thompson, Polytopic ligand directed self-assembly—polymetallic [n×n] grids versus non-grid oligomers, *Chem. Soc. Rev.*, 2009, 38, 2334–2359.
- [34]. M.U. Anwar, L.K. Thompson, L.N. Dawe, F. Habib, M. Murugesu, Predictable self-assembled [2 × 2] Ln(III)<sub>4</sub> square grids (Ln = Dy, Tb)—SMM behaviour in a new lanthanide cluster motif, *Chem. Commun.*, 2012, 48, 4576–4578.
- [35]. A. Bacchi, M. Carcelli, P. Pelagatti, C. Pelizzi, G. Pelizzi, F. Zani, Antimicrobial and mutagenic activity of some carbonyl- and thiocarbonylhydrazone ligands and their copper(II), iron(II) and zinc(II) complexes, *J. Inorg. Biochem.*, 1999, 75, 123–133.
- [36]. A. Bacchi, A. Bonini, M. Carcelli, F. Ferraro, E. Leporati, C. Pelizzi, G. Pelizzi, Chelating behaviour of methyl 2-pyridyl ketone carbonyl- and thiocarbonylhydrazones in copper(II) and zinc(II) complexes, *J. Chem. Soc., Dalton Trans.*, 1996, 2699–2704.
- [37]. P. Novak, T. Jednačak, J. Parlov Vuković, K. Zangger, M. Rubčić, N. Galić, T. Hrenar, Synthesis, Structural Characterization and Hydrogen Bonding of Mono(salicylidene)carbohydrazone, *Croat. Chem. Acta*, 2012, 85, 451–456.
- [38]. P. Akhtar, Z. Yaakob, Y. Ahmed, M. Shahinuzzaman, M.K.M. Hyder, Total Phenolic Contents and Free Radical Scavenging Activity of Different Parts of *Jatropha* Species, *Asian J. Chem.*, 2018, 30, 365–370.
- [39]. O.V. Dolomanov, L.J. Bourhis, R.J. Gildea, J. a. K. Howard, H. Puschmann, OLEX2: a complete structure solution, refinement and analysis program, *J. Appl. Crystallogr.*, 2009, 42, 339–341.
- [40]. G.M. Sheldrick, SHELXT-Integrated space-group and crystal-structure determination, *Acta Crystallogr., Sect. A: Found. Adv.*, 2015, 71, 3–8.
- [41]. G.M. Sheldrick, Crystal structure refinement with SHELXL, *Acta Crystallogr., C: Struct. Chem.* 2015, 71, 3–8.
- [42]. A.R. Božić, N.R. Filipović, T.Ž. Verbić, M.K. Milčić, T.R. Todorović, I.N. Cvijetić, O.R. Klisurić, M.M. Radišić, A.D. Marinković, A detailed experimental and computational study of monocarbonylhydrazones, *Arab. J. Chem.*, 2020, 13, 932–953.
- [43]. G. Mrđan, G. Vastag, D. Škorić, M. Radanović, T. Verbić, M. Milčić, I. Stojiljković, O. Marković, B. Matijević, Synthesis, physicochemical characterization, and TD-DFT calculations of monothiocarbonylhydrazone derivatives, *Struct. Chem.*, 2021, 32, 1231–1245.
- [44]. Y. Kaya, A. Erçağ, Ö. Uğuz, A. Koca, Y. Zorlu, M. Hacıoğlu, A. Seher Birteksöz Tan, New asymmetric bithiocarbonylhydrazones and their mixed ligand nickel(II) complexes: Synthesis, characterization, crystal structure, electrochemical-spectroelectrochemical property, antimicrobial and antioxidant activity, *Polyhedron*, 2021, 207, 115372.
- [45]. Nd. Fall, F.D. Faye, A.A. Gaye, O. Diouf, M. Gaye, Synthesis of mono and bis-substituted asymmetrical compounds, 1-(2'-hydroxy-3'-methoxybenzylidene)carbohydrazone and 1-(2'-hydroxy-3'-methoxybenzylidene)-5-(1'-pyridylmethylene)carbohydrazone: Structural characterization and antioxidant activity study, *J. Appl. Chem.*, 2020, 13, 22–30.
- [46]. A.R. Sayed, H.M.A. El-Lateef, Thiocarbonylhydrazones Based on Adamantane and Ferrocene as Efficient Corrosion Inhibitors for Hydrochloric Acid Pickling of C-Steel, *Coatings*, 2020, 10, 1068.
- [47]. K.G. Sangeetha, K.K. Aravindakshan, Novel ligands, benzophenone N(4)-methyl-N(4)-phenylthiosemicarbazone, 1-(amino-N-methylphenylmethanethio)(diphenylmethylene) thiocarbonylhydrazone and the transition metal complexes of the latter, *Inorg. Chim. Acta*, 2018, 469, 387–396.
- [48]. M. Ndiaye-Gueye, M. Dieng, E.I. Thiam, D. Lo, A.H. Barry, M. Gaye, P. Retailleau, Lanthanide(III) Complexes with Tridentate Schiff Base Ligand, Antioxidant Activity and X-Ray Crystal Structures of the Nd(III) and Sm(III) Complexes, *S. Afr. J. Chem.*, 2017, 70, 8–15.
- [49]. R. Sylla-Gueye, I.E. Thiam, J. Orton, S. Coles, M. Gaye, Crystal structure of N'-[4-(dimethylamino)benzylidene]furan-2-carbohydrazone monohydrate, *Acta Crystallogr., Sect. E: Struct. Chem.*, 2020, 76, 660–663.
- [50]. R. Bikas, P.M. Anarjan, S.W. Ng, E.R.T. Tiekink, 2-[(E)-2-2-[(E)-2-Hydroxybenzylidene]hydrazinecarbonylhydrazinylidene)methyl]phenol, *Acta Crystallogr., Sect. E: Struct. Chem.*, 2012, 68, o193.